


Spectroscopy of the 1001-nm transition in atomic dysprosium

N. Petersen,^{1,2} M. Trümper¹,,¹ and P. Windpassinger^{1,2}

¹*QUANTUM, Institut für Physik, Johannes Gutenberg-Universität, 55099 Mainz, Germany*

²*Graduate School Materials Science in Mainz, Staudingerweg 9, 55128 Mainz, Germany*

 (Received 11 September 2019; revised manuscript received 28 February 2020; accepted 3 March 2020; published 2 April 2020)

We report on spectroscopy of cold dysprosium atoms on the 1001-nm transition and present measurements of the excited-state lifetime which is at least 87(7) ms long. Due to the long excited-state lifetime we are able to measure the ratio of the excited-state polarizability to the ground-state polarizability at 1064 nm to be 0.83(0.13) by parametric heating in an optical dipole trap. In addition we measure the isotope shifts of the three most abundant bosonic isotopes of dysprosium on the 1001-nm transition with an accuracy better than 30 kHz.

DOI: [10.1103/PhysRevA.101.042502](https://doi.org/10.1103/PhysRevA.101.042502)

I. INTRODUCTION

Quantum gases of magnetic atoms enable the study of many-body physics with long-range, anisotropic interactions [1]. Due to their large magnetic moments, especially erbium (Er) and dysprosium (Dy) experiments became more prominent in recent years. This led to the realization of the extended Bose-Hubbard Hamiltonian [2], the observation of the roton mode in the excitation spectrum of a dipolar Bose Einstein condensate [3], and the discovery of self-bound quantum droplets [4,5]. In addition to its large ground-state magnetic moment, Dy features seven stable isotopes of which four have natural abundancies around 20%. Due to its submerged and not completely filled $4f$ -electron shell, its energy spectrum, which is partially depicted in Fig. 1(a), is complex. Among the many possible transitions, there are at least two candidates for ultra-narrow-linewidth ground-state transitions. One at 1322 nm with a predicted lifetime of 6.9 ms and one at 1001 nm with a predicted lifetime of 3 ms [6]. In this work we investigate the latter transition.

Having an ultra-narrow-linewidth transition at hand enriches Dy quantum gas experiments with a versatile tool. Such transitions serve as sensitive probes for interactions between the atoms, for example, on lattice sites of an optical lattice [7] or as probes for the external trapping potential, e.g., to selectively probe different lattice sites in an optical superlattice. Furthermore, because of its long lifetime, the excited state can be used as a second species in the experiment, whose population can be precisely controlled, e.g., to study Kondo-lattice physics [8,9]. Ultra-narrow-linewidth transitions can also be used to probe the inner atomic potentials with a high sensitivity to investigate more fundamental physical questions. It has been proposed to use precise isotope shift measurements of two ultra-narrow-linewidth transitions of the same element to search for high-energy physics contributions to the inner potentials and for physics beyond the standard model [11,12]. In both cases the contributions to the inner potential could reveal themselves as a nonlinearity in a King plot analysis [13] of the two transitions. For this purpose the element needs to have at least four (zero nuclear spin) isotopes, which is

fulfilled by Dy. Recently, the 1001-nm transition has been studied by laser spectroscopy and isotope shifts of all seven stable isotopes had been measured on the 40 MHz accuracy level [14].

The experimental results presented here show that the lifetime of the excited state of the 1001-nm transition with 87(7) ms exceeds the previous theoretical prediction [6]. In addition we refine the precision of the isotope shift measurements to the 30 kHz level for the three most abundant bosonic isotopes and present measurements of the excited-state polarizability at the wavelength of 1064 nm, which is commonly used for optical dipole trapping.

II. EXPERIMENTAL SCHEME

The experimental setup is depicted in Fig. 1(b). A magneto-optical trap (MOT) operated on the $\Gamma_{626} = 2\pi \times 136$ kHz wide transition from the ground state at 626 nm is loaded from a Zeeman slower, which is using the $\Gamma_{421} = 2\pi \times 32$ MHz broad 421-nm transition. Details of the experimental setup can be found in [15]. Typically, 3×10^6 ^{162}Dy or ^{164}Dy atoms or 3×10^5 ^{160}Dy atoms are trapped and cooled to temperatures on the order of 30 μK . The atoms can be transferred to a single beam optical dipole trap (ODT) at 1064 nm. Absorption imaging is done in the horizontal plane in 45° to the ODT beam using the 421-nm transition. The spectroscopy light at 1001 nm is generated by an extended cavity diode laser (ECDL), which is stabilized by the Pound-Drever-Hall method to a cylindrical cavity made of ultralow expansion glass (ULE). We use a fiber EOM and an offset sideband locking technique to shift the laser frequency relative to the cavity resonances, which are spaced by 1.4961935(10) GHz. The ULE cavity is temperature stabilized to the zero-crossing temperature of the coefficient of thermal expansion and we achieve laser linewidths below 1 kHz, and observe drifts of the stabilized laser frequency below 15 kHz/h. The 1001-nm light is scanned in frequency by a double pass acousto-optical modulator (dAOM). The radio frequencies driving the single pass and double pass AOMs and the fiber EOM are generated by direct digital synthesis. The circularly polarized 1001-nm

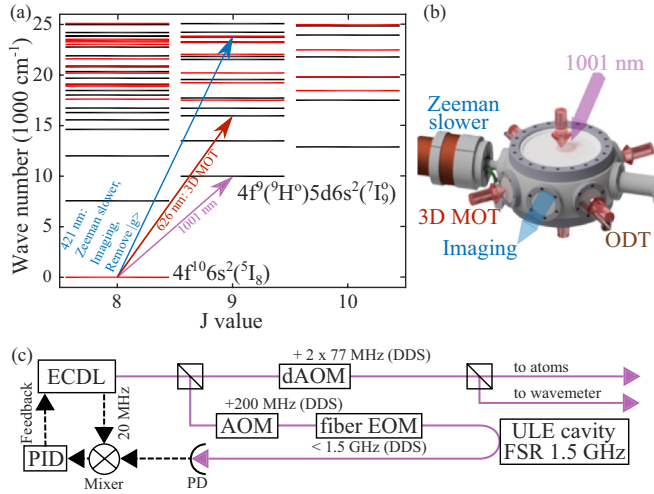


FIG. 1. (a) Excerpt of Dy energy levels for total angular momenta $J = 8, 9,$ and 10 [10]. Even- (odd-) parity levels are drawn in red (black). The electron configuration of the ground state and of the excited state of the 1001-nm transition are written next to the corresponding levels. (b) Experimental setup. (c) 1001-nm laser system. DDS: direct digital synthesis; FSR: free spectral range.

spectroscopy beam is coming from the top of the main chamber under a small angle to the z axis. It is elliptically shaped and has diameters of 9.2 mm and 2.9 mm at the position of the atoms, where the larger half axis of the ellipse points along the ODT beam. From the same direction a resonant 421-nm beam can be applied to the atoms in the ODT to remove all ground-state atoms from the trap. During the application of the spectroscopy pulses the magnetic field at the position of the MOT and the ODT is compensated to zero within the resolution of 626-nm spectroscopy along the imaging axis.

III. MEASUREMENT OF THE ISOTOPE SHIFTS AND ABSOLUTE TRANSITION WAVELENGTH

The spectroscopic measurements to obtain the isotope shifts are carried out in a pulsed manner. Atoms are released from the MOT and after 6 ms time of flight (TOF) a pulse of 6 mW/cm² light at 1001 nm is applied for 12 ms with a fixed detuning to the atomic resonance. After the pulse the remaining ground-state population is measured by absorption imaging and then a new detuning is set and the measurement is repeated. This way the atomic resonance appears as a dip

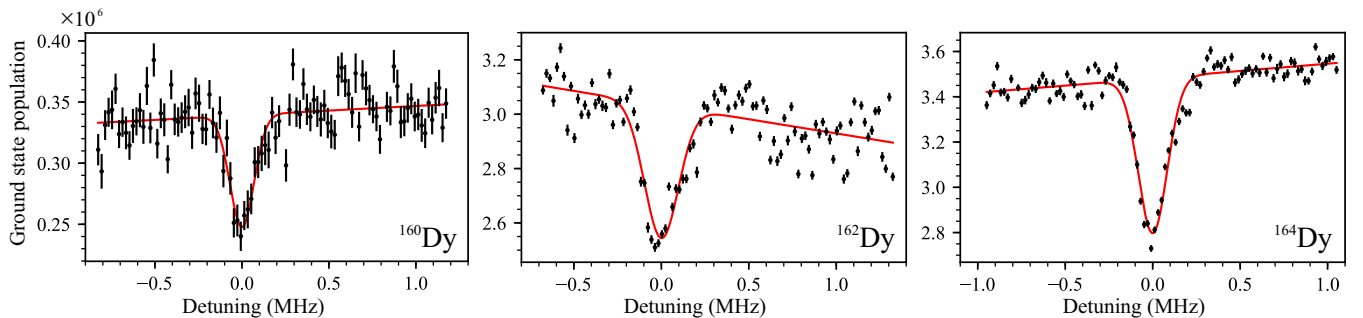


FIG. 2. Exemplary spectra of the 1001-nm transition for ^{160}Dy , ^{162}Dy , and ^{164}Dy .

TABLE I. Summary of uncertainty contributions taken into account for the calculation of the total uncertainty of the measured isotope shifts. rf: radio frequency.

Uncertainty budget contribution	$\delta\nu_{160-164}$ (kHz)	$\delta\nu_{162-164}$ (kHz)
ULE cavity FSR	20	10
ULE frequency drift	14	6.7
rf measurement uncertainty	10	10
Fit uncertainties	7.4	7.8
Total	29	20

in the ground-state population like in the three exemplary spectra presented in Fig. 2. The data points in each spectrum are obtained in sequence. Since there were slow drifts of the overall atom number the background of the spectra exhibits a slope. To determine the atomic resonance frequency from each spectrum an inverted Gaussian function with a linear offset is fitted to the data points. We reference the atomic resonances of ^{160}Dy and ^{162}Dy to the resonance of ^{164}Dy and conduct a ^{164}Dy measurement immediately before and after each measurement of one of the other isotopes. This way we can detect and account for drifts of the ULE cavity, which is the optical frequency reference in our setup. As a result we obtain the following isotope shifts for ^{160}Dy in Eq. (1) and ^{162}Dy in Eq. (2) relative to ^{164}Dy :

$$\delta\nu_{160-164} = -2514.277(29) \text{ MHz}, \quad (1)$$

$$\delta\nu_{162-164} = -1195.773(20) \text{ MHz}. \quad (2)$$

The uncertainty budget is summarized in Table I and takes contributions from ULE cavity FSR uncertainties, ULE frequency drifts, rf measurement uncertainties, and fit uncertainties into account. The rf measurement uncertainty is given by the accuracy of the measurement equipment used to determine the rf frequencies driving the dAOM and fiber EOM. Since the isotope shifts span a frequency range, which is larger than the FSR of the ULE cavity, the laser has to be stabilized to one of three neighboring cavity resonances for the spectroscopy of each isotope. For this reason the uncertainty of the FSR frequency needs to be taken into account. By using a wavelength meter (High Finesse WSU-30), we determine the absolute frequency of the transition for ^{162}Dy to be

$$\nu_{162} = 299.521643(30) \text{ THz} \quad (3)$$

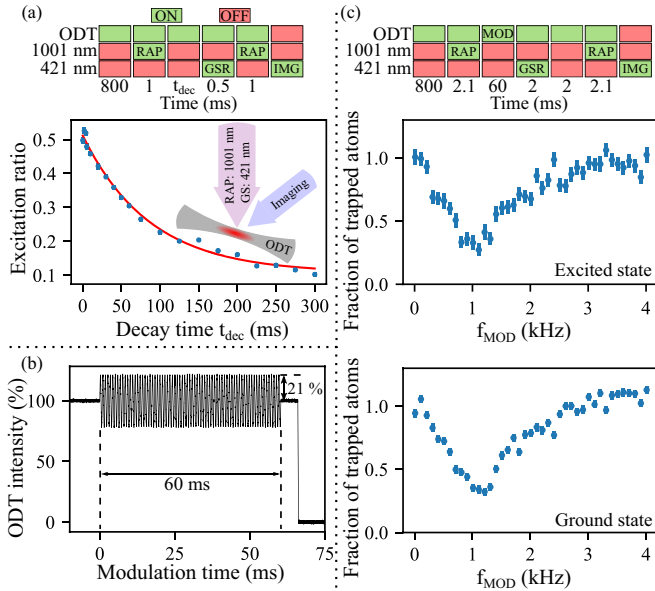


FIG. 3. (a) Measurement sequence for the number of excited-state atoms N_e after a variable holding time, where GSR refers to the resonant 421-nm beam, which is used to remove the ground-state atoms. MOD refers to modulation of the ODT intensity, and IMG to absorption imaging. The blue data points are the measured averaged excitation ratios N_e/N_t versus the holding time after the first RAP in the sequence. The red line is the result of a fit with an exponential decay function with an offset to the data. The lifetime is $\tau_{1001} \geq 87(7)$ ms. Inset: beam setup for the lifetime measurements. (b) Typical ODT intensity modulation at a frequency of $f_{\text{MOD}} = 1210$ Hz. (c) Sequence to measure N_e after 60 ms modulation (MOD) of the ODT intensity. Parametric heating spectra for the excited state (top) and ground state (bottom).

corresponding to a wave number of

$$\tilde{\nu}_{162} = 9990.9666(10) \text{ cm}^{-1}. \quad (4)$$

The accuracy of the rubidium calibrated wavelength meter of 30 MHz is the dominant contribution to the measurement uncertainty by three orders of magnitude.

IV. MEASUREMENT OF THE EXCITED-STATE LIFETIME

The lifetime of the excited state is measured by the following sequence, which is outlined in Fig. 3(a). About 2.1×10^5 ^{162}Dy atoms are trapped in the ODT after a holding time of 800 ms. By applying a linear ramp of the laser detuning from -300 kHz below the atomic resonance to 300 kHz above the atomic resonance in $984 \mu\text{s}$ with 4.88 Hz wide frequency steps and with a peak intensity of $450 \text{ mW}/\text{cm}^2$ about 71% of the ground-state population is transferred to the excited state of the 1001-nm transition by means of a rapid adiabatic passage (RAP). The mixture of ground- and excited-state atoms is trapped for a variable amount of time between 0.01 ms and 300 ms during which excited-state atoms can decay back to the ground state. After this variable holding time, resonant 421-nm light is applied to remove the ground-state population. Then another RAP transfers 71% of the excited-state atoms back to the ground state and subsequently the ground-state

atom number N_e is measured by absorption imaging which is proportional to the number of excited-state atoms before the second RAP pulse was applied. This sequence is repeated without applying the RAP pulses and the ground state removing 421-nm beam to obtain the total atom number N_t . For each holding time N_e and N_t are measured 15 times in turns and the resulting excitation ratios N_e/N_t are averaged. The decay of the excitation ratio is plotted in Fig. 3(a). The order in which the excitation ratio was measured for different holding times was randomized. By fitting an exponential decay function with an offset to the data we find the lifetime of the excited state to be

$$\tau_{1001} \geq 87(7) \text{ ms}. \quad (5)$$

This is a lower limit for the lifetime since other effects that could decrease the excited-state population over time like inelastic collisions between ground- and excited-state atoms and between pairs of excited-state atoms might be present. In comparative measurements with a similar initial atomic density in the ODT the ground-state population has a lifetime of at least 2.6 s. By keeping the 1001-nm beam constantly on and on resonance with the transition the trap lifetime of the ground state is reduced to about 200 ms, where also a dependence of the loss rate on the atomic density is observed. We suppose inelastic collisions between ground- and excited-state atoms lead to increased density dependent losses from the ODT for both states and we account for these in the fitting procedure. Compared to the theoretical prediction of $\tau_{1001, \text{theor}} = 3$ ms the measured excited-state lifetime is almost a factor 30 longer than expected [6].

V. MEASUREMENT OF THE EXCITED-STATE POLARIZABILITY

Since the excited-state lifetime is more than one order of magnitude larger than expected we are able to use parametric heating [16–18] of excited-state atoms in the ODT to measure the ratio of the excited-state dynamic polarizability α_e to the ground-state dynamic polarizability α_g at 1064 nm. For this purpose the intensity of the ODT beam is modulated for 60 ms with an amplitude of 21% [Fig. 3(b)] and modulation frequencies f_{mod} ranging from 10 Hz to 4010 Hz. The horizontal [vertical] beam radius is $w_h = 28.3(5.9) \mu\text{m}$ [$w_v = 58.3(4.6) \mu\text{m}$] at the position of the atoms and the beam power is approximately 11 W. In the case of the excited state the sequence depicted in Fig. 3(c) is applied, where the ODT intensity modulation is switched on after a RAP transfers about 62% of the atoms to the excited state. Then the ground-state atoms are removed by resonant 421-nm light before a second RAP transfers part of the excited-state population to the ground state and an absorption image is taken. The parametric heating spectrum for excited-state atoms is depicted in Fig. 3(c) on the top and features a resonance at $f_e = 1.043(60)$ kHz. Due to depletion of our atomic beam source the total ground-state population is reduced to about 20×10^3 atoms in the ODT. The parametric heating resonance for ground-state atoms under the same trapping conditions is measured by using the same sequence as for the excited state but without applying the RAPs and the resonant 421-nm light. The resulting spectrum is depicted in the lower half of

Fig. 3(c) and it shows a resonance at $f_g = 1.146(60)$ kHz. Since the analytic function which describes the parametric heating spectrum is not known, we restricted the analysis to the determination of the minima of the resonance features by fitting third-order polynomial functions to a 800-Hz-wide region. The uncertainties stated for f_g and f_e are the statistical uncertainties of the fits. Systematic uncertainties due to not knowing the exact underlying line shape might be higher. However, we can limit the systematic uncertainty of the relative resonance positions at least in one direction. It is obvious that f_g and f_e are close to each other compared to the width of the resonances. From the sign of the light shifts of the transition for different ODT beam powers, which is described below, we can deduce that f_e has to be lower than f_g as observed in the spectra in Fig. 3(c) and determined by the fits. From the resonances we obtain the ratio of the polarizabilities analog to [19]:

$$\alpha_e/\alpha_g = (f_e/f_g)^2 = 0.83(0.13). \quad (6)$$

Theoretical calculations lead to $\alpha_e/\alpha_g = 157$ a.u./181 a.u. = 0.870 [20], while for the ground state

$$\alpha_g = 184.4(2.4) \text{ a.u.} \quad (7)$$

is the experimentally determined value [19]. From Eq. (6) and Eq. (7) we then obtain

$$\alpha_e = 153(24) \text{ a.u.} \quad (8)$$

for the excited-state polarizability. The above results are in a good approximation independent of the exact trapping beam parameters if the ground- and excited-state populations are having similar density distributions in the trap and thus experience similar anharmonicity and beam aberrations. Obtaining precise values for the beam radii at the position of the atoms is difficult and usually prone to large relative errors. The above stated values for w_h and w_v were obtained from standard beam analysis with an attenuated ODT beam on a CCD camera and can have larger systematic errors than stated above. Nevertheless, we perform a measurement of the 1001-nm line shift for varying ODT beam powers and calculate the difference in

polarizabilities to be

$$\Delta\alpha = \alpha_e - \alpha_g = \frac{hc}{4a_0^3} w_h w_v m_s = -21.5(5.0) \text{ a.u.}, \quad (9)$$

where h is the Planck constant, c is the speed of light, a_0 is the Bohr radius, and $m_s = -38.9(2.4)$ kHz/W is the observed slope of the line shift per beam power. A reduction of the mean intensity experienced by the atoms due to their spread around the potential minimum is taken into account in the form of a correction factor in the calculation of m_s . With Eq. (7) we obtain $\alpha_e = 162.9(5.5)$ a.u. Since the vector and tensor polarizabilities of both states are expected to be two orders of magnitude smaller than the scalar polarizabilities, dependencies on ODT beam polarization and the atomic azimuthal quantum number were neglected in the considerations [19,21].

VI. CONCLUSIONS

We have measured the relative isotope shifts of the three most abundant bosonic isotopes of dysprosium on the 1001-nm transition with an accuracy better than 30 kHz, while the absolute frequencies were determined with an uncertainty of 30 MHz. In addition, we have determined a lower boundary for the excited-state lifetime, which is more than one order of magnitude larger than expected from theoretical predictions [6]. The dynamical polarizability of the excited state was determined relative to the ground-state dynamical polarizability and the ratio is in fair agreement with theory [20].

ACKNOWLEDGMENTS

The authors would like to thank F. Mühlbauer, L. Maske, G. Türk, and C. Baumgärtner for their contributions to the experiment and the group of K. Wendt for their support, advice, and joint use of their wavelength meter. We thank D. Budker for his very appreciated advice during the initial search for the 1001-nm transition. We gratefully acknowledge financial support by the DFG-Grossgerät Grant No. INST 247/818-1 FUGG and the Graduate School of Excellence MAINZ (Grant No. GSC 266).

-
- [1] T. Lahaye, C. Menotti, L. Santos, M. Lewenstein, and T. Pfau, The physics of dipolar bosonic quantum gases, *Rep. Prog. Phys.* **72**, 126401 (2009).
 - [2] S. Baier, M. J. Mark, D. Petter, K. Aikawa, L. Chomaz, Z. Cai, M. Baranov, P. Zoller, and F. Ferlaino, Extended Bose-Hubbard models with ultracold magnetic atoms, *Science* **352**, 201 (2016).
 - [3] L. Chomaz, R. M. W. Bijnen, D. Petter, G. Faraoni, S. Baier, J. H. Becher, M. J. Mark, F. Waechtler, L. Santos, and F. Ferlaino, Observation of roton mode population in a dipolar quantum gas, *Nat. Phys.* **14**, 442 (2018).
 - [4] I. Ferrier-Barbut, H. Kadau, M. Schmitt, M. Wenzel, and T. Pfau, Observation of Quantum Droplets in a Strongly Dipolar Bose Gas, *Phys. Rev. Lett.* **116**, 215301 (2016).
 - [5] M. Schmitt, M. Wenzel, F. Böttcher, I. Ferrier-Barbut, and T. Pfau, Self-bound droplets of a dilute magnetic quantum liquid, *Nature (London)* **539**, 259 (2016).
 - [6] V. A. Dzuba and V. V. Flambaum, Theoretical study of some experimentally relevant states of dysprosium, *Phys. Rev. A* **81**, 052515 (2010).
 - [7] F. Scazza, C. Hofrichter, M. Höfer, P. C. De Groot, I. Bloch, and S. Fölling, Observation of two-orbital spin-exchange interactions with ultracold SU(N)-symmetric fermions, *Nat. Phys.* **10**, 779 (2014).
 - [8] M. Foss-Feig, M. Hermele, and A. M. Rey, Probing the Kondo lattice model with alkaline-earth-metal atoms, *Phys. Rev. A* **81**, 051603 (2010).
 - [9] L. Riegger, N. D. Oppong, M. Höfer, D. R. Fernandes, I. Bloch, and S. Fölling, Localized Magnetic Moments with Tunable Spin Exchange in a Gas of Ultracold Fermions, *Phys. Rev. Lett.* **120**, 143601 (2018).
 - [10] A. Kramida, Yu. Ralchenko, J. Reader, and NIST ASD Team, NIST Atomic Spectra Database (ver. 5.5.6) (online), National Institute of Standards and Technology, Gaithersburg, MD, 2018, <https://physics.nist.gov/asd>.

- [11] C. Delaunay, R. Ozeri, G. Perez, and Y. Soreq, Probing atomic Higgs-like forces at the precision frontier, *Phys. Rev. D* **96**, 093001 (2017).
- [12] K. Mikami, M. Tanaka, and Y. Yamamoto, Probing new intra-atomic force with isotope shifts, *Eur. Phys. J. C* **77**, 896 (2017).
- [13] W. H. King, Comments on the article “Peculiarities of the isotope shift in the Samarium spectrum”, *JOSA* **53**, 638 (1963).
- [14] D. Studer, L. Maske, P. Windpassinger, and K. Wendt, Laser spectroscopy of the 1001-nm ground-state transition in dysprosium, *Phys. Rev. A* **98**, 042504 (2018).
- [15] F. Mühlbauer, N. Petersen, C. Baumgärtner, L. Maske, and P. Windpassinger, Systematic optimization of laser cooling of dysprosium, *Appl. Phys. B* **124**, 120 (2018).
- [16] M. E. Gehm, K. M. O’hara, T. A. Savard, and J. E. Thomas, Dynamics of noise-induced heating in atom traps, *Phys. Rev. A* **58**, 3914 (1998).
- [17] R. Jáuregui, Nonperturbative and perturbative treatments of parametric heating in atom traps, *Phys. Rev. A* **64**, 053408 (2001).
- [18] S. Friebel, C. D’Andrea, J. Walz, M. Weitz, and T. W. Hänsch, CO₂-laser optical lattice with cold rubidium atoms, *Phys. Rev. A* **57**, R20 (1998).
- [19] C. Ravensbergen, V. Corre, E. Soave, M. Kreyer, S. Tzanova, E. Kirilov, and R. Grimm, Accurate Determination of the Dynamical Polarizability of Dysprosium, *Phys. Rev. Lett.* **120**, 223001 (2018).
- [20] V. A. Dzuba, V. V. Flambaum, and B. L. Lev, Dynamic polarizabilities and magic wavelengths for dysprosium, *Phys. Rev. A* **83**, 032502 (2011).
- [21] H. Li, J.-F. Wyart, O. Dulieu, S. Nascimbène, and M. Lepers, Optical trapping of ultracold dysprosium atoms: transition probabilities, dynamic dipole polarizabilities and van der Waals C₆ coefficients, *J. Phys. B* **50**, 014005 (2017).